Deformable Self-Propelled Particles

Takao Ohta* and Takahiro Ohkuma†

Department of Physics, Graduate School of Science, Kyoto University, Kyoto 606-8502, Japan

(Received 8 October 2008; published 13 April 2009)

A theory of self-propelled particles is developed in such a way that the particles can be deformed from a circular shape when the propagating velocity is finite. A coupled set of equations in terms of the velocity and a tensor variable is introduced to represent the motion of a deformed particle. It is shown that there is a bifurcation from a straight motion to a circular motion by increasing the propagating velocity. The dynamics of assembly of the particles is studied numerically in two dimensions imposing a global interaction such that the elongated particles tend to undergo an orientational order.

DOI: 10.1103/PhysRevLett.102.154101 PACS numbers: 05.45.−a, 05.40.Jc, 05.70.Ln, 82.40.Ck

Individual and collective dynamics of self-propelled objects are one of the fundamental problems in nonequilibrium physics. There have been a number of studies for many years based on both deterministic dynamics [1,2] and stochastic dynamics [3–8]. Recently the hydrodynamic effects with and without internal degrees of freedom have been investigated intensively [9–12]. Motion of a droplet or a vesicle moving under the interaction with substrate has been studied [13–15]. Experiments of reaction-driven propulsion [16,17] as well as a theory [18] and computer simulations [19,20] have been carried out recently. Excitable reaction diffusion systems have also exhibited self-propelled domains [21] and have been analyzed theoretically [22–24]. These studies are motivated, on the one hand, to gain an understanding of macroscopic self-organization far from equilibrium and, on the other hand, to clarify the mechanism of molecular machines in mesoscopic or nanoscopic length scales.

All of the above studies except for the model with internal degrees of freedom such as a dimmer model [12] assume that the particle shape is unchanged during the motion. In reality, however, many self-propelled objects may change their shape depending on the velocity or the interaction with other objects. Biological systems such as living cells are one example [25,26]. The excitable reaction diffusion system provides another example. The numerical results in Ref. [21] clearly show that a two-dimensional excited pulse changes its shape as the propagating velocity increases.

The purpose of this Letter is to investigate the individual and the collective motions of self-propelled deformable particles. It will be shown that a competition between a circular motion of individual particles and an orientational order of their shape due to a global interaction causes a rich variety of collective dynamics.

In order to represent the motion of a two-dimensional deformable particle with a coupling between the velocity of the center of the gravity and the deformation around a circular shape, we introduce two variables. One is the velocity $\boldsymbol{v} = (v_1, v_2)$ of the center of gravity and the other is a tensor $S_{\alpha\beta}$ with $(\alpha, \beta = 1, 2)$. Suppose that the deformation is weak and each deformed particle takes an elliptical shape. We define a unit vector $\boldsymbol{n}$ along the long axis as shown in Fig. 1. The tensor $S_{\alpha\beta}$, which is the same as the nematic order parameter [27], is given in terms of the components of $\boldsymbol{n}$ by

$$S_{\alpha\beta} = s(n_\alpha n_\beta - \tfrac{1}{2}\delta_{\alpha\beta}), \tag{1}$$

which is normalized as $\mathrm{Tr}S = 0$ and the positive constant s represents the degree of deformation from a circular shape.

The time-evolution equations for $\boldsymbol{v}$ and $S_{\alpha\beta}$ can be derived by a symmetry argument as follows. First of all, the velocity should obey in its simplest case

$$\frac{d}{dt}v_\alpha = \gamma v_\alpha - |\boldsymbol{v}^2|v_\alpha - aS_{\alpha\beta}v_\beta, \tag{2}$$

where the repeated indices imply summation. The first and the second terms are the same as those of an active Brownian particle [4–6]. In particular, Schweitzer *et al.* introduced a model system for active particles where the velocity obeys a force balance equation which is coupled with an internal energy depot [4]. After eliminating the depot variable adiabatically and employing an expansion in terms of $\boldsymbol{v}$, one obtains Eq. (2) without the last term. Note that when the energy input is smaller than the threshold value, i.e., $\gamma < 0$, the particle does not move, whereas when $\gamma > 0$, the particle undergoes self-propelled motion. Throughout this Letter, we assume that $\gamma > 0$. The combination $S_{\alpha\beta}v_\beta$ with a scalar coefficient a as the last term of

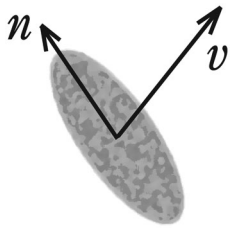

FIG. 1. Self-propelled particle with the velocity $\boldsymbol{v}$ and the unit normal $\boldsymbol{n}$ along the long axis.

(2) is the simplest way to constitute a vector variable in terms of $\boldsymbol{v}$ and $S_{\alpha\beta}$. Similarly, by symmetry, the tensor $v_\alpha v_\beta - \frac{1}{2}|\boldsymbol{v}^2|\delta_{\alpha\beta}$ should enter into the time-evolution equation for $S_{\alpha\beta}$

$$\frac{d}{dt}S_{\alpha\beta} = -\kappa S_{\alpha\beta} + b\left(v_\alpha v_\beta - \frac{1}{2}|\boldsymbol{v}^2|\delta_{\alpha\beta}\right), \tag{3}$$

where $\kappa > 0$ and b are constant. Since $\mathrm{Tr}S = 0$, the area of a particle is conserved.

By writing the velocity as $v_1 = v\cos\phi$, $v_2 = v\sin\phi$ and the unit normal as $n_1 = \cos\theta$ and $n_2 = \sin\theta$, Eqs. (2) and (3) are rewritten as

$$\frac{d}{dt}v = v(\gamma - v^2) - \frac{1}{2}asv\cos 2(\theta - \phi) \tag{4}$$

$$\frac{d}{dt}\phi = -\frac{1}{2}as\sin 2(\theta - \phi) \tag{5}$$

$$\frac{d}{dt}s = -\kappa s + v^2 b\cos 2(\theta - \phi) \tag{6}$$

$$\frac{d}{dt}\theta = -\frac{v^2 b}{2s}\sin 2(\theta - \phi), \tag{7}$$

where v and s should be positive. From Eqs. (5) and (7), one obtains for $\psi = \theta - \phi$

$$\frac{d}{dt}\psi = -\frac{1}{2}\left(-as + \frac{bv^2}{s}\right)\sin 2\psi. \tag{8}$$

It is noted that only the difference ψ of the two angles enters into the time-evolution equations due to the spatial isotropy.

The above set of equations has a stationary solution. Without loss of generality, we may assume that the velocity is parallel to the x axis, i.e., $\phi = 0$. There are two kinds of solution depending on the sign of the parameter b. When b is positive, the stationary solution is given by $\theta = 0$, $v^2 = v_0^2 = \gamma/(1 + B)$, and $s = s_0 = bv_0^2/\kappa$, where $B \equiv ab/(2\kappa)$. When b is negative, the solution is given by $\theta = \pi/2$, $v = v_0$, and $s = -s_0$. In the latter case, the long axis of the elliptical particle is perpendicular to the velocity vector. In order to avoid a singular behavior of v_0 for $B \leq -1$, we hereafter assume $ab > 0$ ($B > 0$).

We apply a linear stability analysis of the stationary solutions. It is readily shown that the stability is solely determined by Eq. (8). The stationary solution is stable when the coefficient on the right-hand side of Eq. (8) is negative, i.e., $abv_0^2 \leq \kappa^2$. Therefore the threshold is given by

$$\gamma = \gamma_c = \frac{\kappa^2}{ab} + \frac{\kappa}{2}. \tag{9}$$

When $\gamma \geq \gamma_c$, the stationary straight motion becomes unstable. Note that this is valid for both $\theta = 0$ and $\theta = \pi/2$. This bifurcation threshold is indicated on the γ-κ plane in Fig. 2.

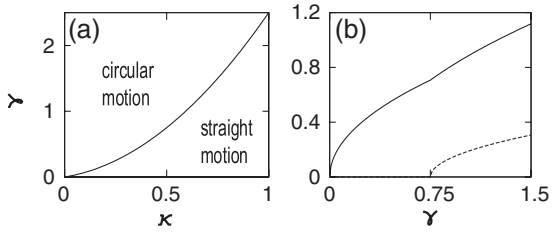

FIG. 2. (a) Stability diagram on the γ-κ plane for $ab = 0.5$. (b) The velocity v (full line) and the frequency ω (broken line) as a function of γ for $a = -1.0$, $b = -0.5$, and $\kappa = 0.5$. The bifurcation occurs at $\gamma_c = 0.75$.

Now we investigate the dynamics of a self-propelled particle when the steady solution v_0 and s_0 of a straight motion becomes linearly unstable. Here we make an ansatz that there occurs a circular motion and explore the stability both numerically and analytically. To this end, we put $v = v_r$, $s = s_r$ and $\theta = \omega t + \zeta/2$ and $\phi = \omega t$. Substituting these into Eqs. (4)–(7), one obtains after some algebra

$$v_r^2 = \gamma - \frac{\kappa}{2} \tag{10}$$

and $s_r^2 = bv_r^2/a$, $\cos\zeta = \kappa/as_r$, and $\omega^2 = (ab/4)\times(v_r^2 - v_c^2)$, where $v_c = \kappa/(ab)^{1/2}$. The frequency ω continuously increases from zero at $\gamma = \gamma_c$. It is readily shown that v is also continuous at the bifurcation point $\gamma = \gamma_c$. The γ dependence of v and ω is displayed in Fig. 2(b).

In order to study the dynamics near the bifurcation $\gamma = \gamma_c$ in more detail, we make a reduction of the variables. Note that the coefficient of Eq. (8) vanishes at the bifurcation point. Therefore, the variable ψ is slow near the stability threshold compared to the other variables v and s. This allows us to eliminate these variables by putting $dv/dt = ds/dt = 0$ in Eqs. (4) and (6). As a result, Eq. (8) becomes

$$\frac{d}{dt}\psi = F(\psi) = -\kappa\left[\frac{\gamma - \gamma_c + (\kappa/2 - \gamma)(1 - \cos^2 2\psi)}{-2\gamma_c + \kappa(1 - \cos^2 2\psi)}\right]\tan 2\psi. \tag{11}$$

The function $F(\psi)$ is an odd function since both clockwise and counterclockwise circular motions are equally possible. It is readily verified that Eq. (11) for $-\pi/2 < \psi < \pi/2$ is monostable for $\gamma \leq \gamma_c$ whereas it becomes bistable for $\gamma \geq \gamma_c$. Therefore the change of the stability occurs as a pitchfork bifurcation.

The linear stability of the circular motion is studied numerically by evaluating the eigenvalues of the linearized equations of (4), (6), and (8). It turns out that the stability threshold coincides with that of the straight motion given in Fig. 2. This implies that in the region where the straight

steady motion is stable, the circular motion is unstable and vice versa.

Here we make a remark that we have carried out preliminary numerical simulations in three dimensions extending the model equations (2) and (3) to arbitrary dimensions and have found a stable helical motion of a deformed particle.

It is mentioned that a model of self-propelled particle which exhibits a circular motion has been introduced quite recently by van Teeffelen and Loewen [28]. However, their model does not have a bifurcation from a straight motion to a circular motion shown above.

Now we explore the collective motion of the deformable particles. We introduce a global coupling such that

$$\frac{d}{dt}S_{\alpha\beta}^{(n)} = -\kappa S_{\alpha\beta}^{(n)} + b\left(v_\alpha^{(n)}v_\beta^{(n)} - \frac{1}{2}(\boldsymbol{v}^{(n)})^2\delta_{\alpha\beta}\right) - \hat{K}(S_{\alpha\beta}^{(n)} - \bar{S}), \tag{12}$$

where $\bar{S} = (1/N)\sum_n S_{\alpha\beta}^{(n)}$ and $\hat{K}$ is the coupling constant. The superscript n means the nth particle. The total number of the particles is denoted by N. Equation (12) should be coupled with Eq. (2) in which v_α and $S_{\alpha\beta}$ are replaced, respectively, by $v_\alpha^{(n)}$ and $S_{\alpha\beta}^{(n)}$. The last term in Eq. (12) with a positive value of $\hat{K}$ implies that the elliptical particles tend to make an orientational order. It is mentioned that an orientational order has been studied in self-locomoting rods which are not deformable [29].

We have investigated the motion of the particles numerically in the situation such that individual particles undergo a circular motion when $\hat{K} = 0$. The parameters are fixed as $a = -1.0$, $b = -0.5$, $\kappa = 0.5$, and $\gamma = 1.0$, whereas the interaction strength $K = \hat{K}/\kappa$ is varied. The number of the particles is chosen as $N = 30$ in most of the numerical simulations.

Figure 3 displays the trajectory of a particle for four different values of K. When K is small as $K = 0.14$, the motion is almost circular and localized as in Fig. 3(a). A transition to a delocalized state occurs around at $K = 0.15$. A random drift motion appears as in Fig. 3(b). For larger values of K, a random but ballistic motion becomes dominant as shown in Fig. 3(c). When K exceeds 0.30, each particle exhibits a straight motion as displayed in Fig. 3(d).

In order to analyze the above behavior of the collective motion, we have evaluated the Lyapunov exponent L defined through the relation

$$\exp(L(t - t_0)/\tau) = \sum_{n=1}^{N}\{[\boldsymbol{v}^{(n)}(t) - \hat{\boldsymbol{v}}^{(n)}(t)]^2 - \det[S^{(n)}(t) - \hat{S}^{(n)}(t)]\}, \tag{13}$$

where $\tau = 2\pi/\omega = 8\sqrt{2}\pi \approx 35.5$ for the present set of the parameter values. Small noises of the order of 10^{-4} are added for the hat-marked variables at $t_0 = 3200$. The exponent L is obtained by changing the value of K and is

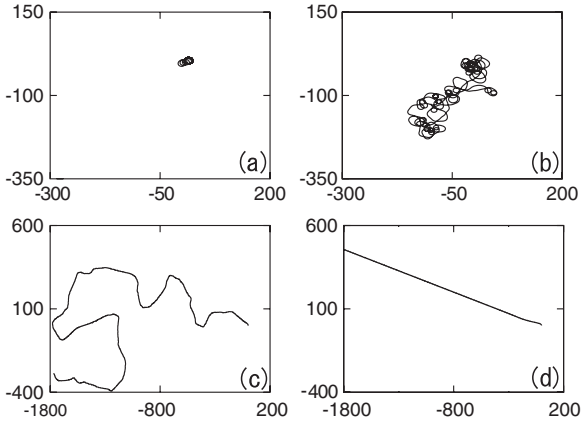

FIG. 3. Trajectory of a particle for (a) $K = \hat{K}/\kappa = 0.14$ and for the time interval $\delta t = 5000$, (b) $K = 0.16$ and for $\delta t = 5000$, (c) $K = 0.28$ and for $\delta t = 5000$, and (d) $K = 0.32$ and for $\delta t > 2000$. Note that (c) and (d) cover a wider area than (a) and (b).

shown in Fig. 4(a). The Lyapunov exponent is almost zero for $K \leq 0.14$ and $K \geq 0.3$, whereas it is definitely positive for $0.15 \leq K \leq 0.29$. Therefore we conclude that the motion is chaotic in this parameter regime. In Fig. 4(a), the data of 100 independent runs are plotted. The vertical bars indicate the typical scatter of the data. The reason why the exponent is not negative but zero in the nonchaotic region is that there is a zero eigenmode in the time-evolution equations due to the rotational invariance.

In order to quantify the distinct dynamics shown above, we have calculated the mean square displacement W averaged over 30 particles

$$W = \left[\frac{1}{N}\sum_{n=1}^{N}\left(\int_0^t \boldsymbol{v}^{(n)}(t')dt'\right)^2\right]^{1/2}. \tag{14}$$

Since there is a crossover from a random drift to a ballistic motion of a particle as is evident in Fig. 3, we assume the time dependence of W for sufficiently large values of t as

$$W = 2D(t/\tau)^{1/2} + Bt/\tau. \tag{15}$$

The diffusion constant D defined through the relation (15)

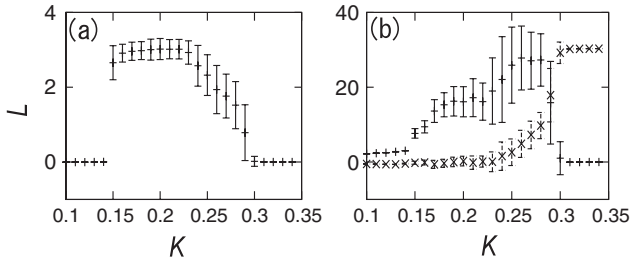

FIG. 4. (a) Lyapunov exponent as a function of the interaction strength K. (b) Diffusion constant D (plus) and the coefficient B (cross) in Eq. (15) as a function of the interaction strength K. These are obtained from 100 independent runs.

is plotted in Fig. 4(b) as a function of the interaction strength K. It is clearly seen that the diffusion constant starts to increase in the chaotic region of $K \geq 0.15$ and becomes zero for $K \geq 0.3$, whereas the value of B starts to increase at $K \geq 0.25$ as shown in Fig. 4(b) indicating that a ballistic-type behavior appears.

In summary, we have introduced and studied a kinetic model for deformable self-propelled particles. It is found that an isolated particle exhibits a bifurcation such that a straight motion becomes unstable and a circular motion appears. Here we make a remark that a similar bifurcation is shown to exist in a model system in Ref. [30], but a circular motion appears in an unrealistic parameter region.

Assembly of the elliptically deformed particles exhibits curious dynamics when the global orientational coupling is introduced. It is found that three phases emerge by increasing the interaction strength, i.e., the localized phase, delocalized chaotic phase, and the phase of the ballistic motion. The change between chaotic and nonchaotic dynamics occurs as a sharp transition, whereas the change from the diffusion to the ballistic motion is a gradual crossover. The final ballistic phase can be understood easily. When the direction of the velocity and hence the orientation of each particle are random, the average $\bar{S}$ is zero in Eq. (12) so that this equation is decoupled for each particle. The damping constant κ is renormalized as $\kappa + \hat{K}$ and hence, for large values of $\hat{K}$, the system enters in the phase of a straight motion in Fig. 2(a).

It is expected qualitatively that the chaotic dynamics in the intermediate strength of the coupling constant K originates from a competition between the circular motion of individual particles and the tendency of the orientation order. The coexistence of clockwise and counterclockwise motions plays a crucial role for the chaotic dynamics since it tends to interrupt the orientational order and to cause a frustration. In this respect, noise effects might be interesting. When noises are strong enough, they should switch randomly from a counterclockwise motion to a clockwise motion and vise versa. In order to examine this, we have added a noise term ξ in Eq. (2), which obeys the Gaussian white statistics, i.e., $\langle \xi(t) \rangle = 0$ and $\langle \xi(t)\xi(s) \rangle = 2M\delta(t - s)$ with a positive constant M, and have carried out numerical simulations for the parameters $a = \gamma = 1$ and $b = \kappa = 0.5$. The switching behavior is found to be frequent for $M \geq 0.005$.

Finally, it is noted that our preliminary numerical simulations have verified that the above property of the complex collective dynamics is essentially unchanged when an attractive interaction is introduced, whose strength is proportional to the distance of a pair of particles. The full account of these results together with the stochastic dynamics under noises and the motion in three dimensions will be published elsewhere in the near future.

This work was supported by the Grant-in-Aid for the priority area ''Soft Matter Physics'' from the Ministry of Education, Culture, Sports, Science and Technology (MEXT) of Japan.

*takao@scphys.kyoto-u.ac.jp
†ohkuma@ton.scphys.kyoto-u.ac.jp

[1] H. Levine, W-J. Rappel, and I. Cohen, Phys. Rev. E **63**, 017101 (2000).
[2] Y-l, Chuang, M. R D'Orsogna, D. Marthaler, A. L. Bertozzi, and L. S. Chayes, Physica (Amsterdam) **232D**, 33 (2007).
[3] T. Vicsek *et al.*, Phys. Rev. Lett. **75**, 1226 (1995).
[4] F. Schweitzer, W. Ebeling, and B. Tilch, Phys. Rev. Lett. **80**, 5044 (1998).
[5] C. A. Condat and G. J. Sibona, Physica (Amsterdam) **168–169D**, 235 (2002).
[6] W. Ebeling and I. M. Sokolov, *Statistical Thermodynamics and Stochastic Theory of Nonequilibrium Systems* (World Scientific, London, 2005).
[7] G. Gregoire and H. Chate, Phys. Rev. Lett. **92**, 025702 (2004).
[8] F. Peruani and L. G. Morelli, Phys. Rev. Lett. **99**, 010602 (2007).
[9] R. A. Simha and S. Ramaswamy, Phys. Rev. Lett. **89**, 058101 (2002).
[10] I. Llopis and I. Pagonabarraga, Europhys. Lett. **75**, 999 (2006).
[11] I. S. Aranson *et al.*, Phys. Rev. E **75**, 040901(R) (2007).
[12] G. P. Alexander and J. M. Yeomans, Europhys. Lett. **83**, 34 006 (2008).
[13] I. Durand, P. Jonson, C. Misbah, A. Valance, and K. Kassner, Phys. Rev. E **56**, R3776 (1997).
[14] L. M. Pismen, Phys. Rev. E **74**, 041605 (2006).
[15] U. Thiele and E. Knobloch, Phys. Rev. Lett. **97**, 204501 (2006).
[16] M. Nagayama *et al.*, Physica (Amsterdam) **194D**, 151 (2004).
[17] Y. Sumino and K. Yoshikawa, Chaos **18**, 026106 (2008).
[18] K. John *et al.*, Eur. Phys. J. E **18**, 183 (2005).
[19] R. Golestanian *et al.*, Phys. Rev. Lett. **94**, 220801 (2005).
[20] Y-G. Tao and R. Kapral, J. Chem. Phys. **128**, 164518 (2008).
[21] K. Krischer and A. Mikhailov, Phys. Rev. Lett. **73**, 3165 (1994).
[22] M. Or-Guil *et al.*, Phys. Rev. E **57**, 6432 (1998).
[23] T. Ohta, Physica (Amsterdam) **151D**, 61 (2001).
[24] Y. Nishiura *et al.*, Chaos **15**, 047509 (2005).
[25] T. Killich *et al.*, J. Cell Sci. **106**, 1005 (1993).
[26] P. Dieterich *et al.*, Proc. Natl. Acad. Sci. U.S.A. **105**, 459 (2008).
[27] P. G. de Gennes and J. Prost, *The Physics of Liquid Crystals* (Oxford University, Oxford, 1993).
[28] S. van Teeffelen and H. Lowen, Phys. Rev. E **78**, 020101 (R) (2008).
[29] D. Saintillan and M. J. Shelley, Phys. Rev. Lett. **99**, 058102 (2007).
[30] N. Shimoyama *et al.*, Phys. Rev. Lett. **76**, 3870 (1996).